
MUON+: Towards Better Muon via One Additional Normalization Step

Ruijie Zhang, Yequan Zhao, Ziyue Liu, Zhengyang Wang, Zheng Zhang[†]
University of California at Santa Barbara
{ruijiezhang, yequanzhao, ziyueliu, zhengyangwang}@ucsb.edu,
zhengzhang@ece.ucsb.edu

Abstract

The Muon optimizer has demonstrated promising performance in pre-training large language models through gradient (or momentum) orthogonalization. In this work, we propose a simple yet effective enhancement to Muon, namely **MUON+**, which introduces an additional normalization step after orthogonalization. We demonstrate the effectiveness of MUON+ through extensive pre-training experiments across a wide range of model scales and architectures. Our evaluation includes GPT-style models ranging from 130M to 774M parameters and LLaMA-style models ranging from 60M to 1B parameters. We comprehensively evaluate the effectiveness of MUON+ in the compute-optimal training regime and further extend the token-to-parameter (T2P) ratio to an industrial level of ≈ 200 . Experimental results show that MUON+ provides a consistent boost on training and validation perplexity over Muon. We provide our code here: <https://github.com/K1seki221/MuonPlus>.

1 Introduction

Based on the empirical observation of scaling laws [12, 10, 16], powerful foundation models such as GPT, DeepSeek, LLaMA, and Gemini [1, 22, 6, 31] have been trained and widely deployed. Nevertheless, as the sizes of both model parameters and training datasets reach extreme levels, the computational cost of pre-training has become prohibitively high. This challenge has motivated increasing research dedicated to improving pre-training efficiency [27, 8, 35, 40, 38, 25], with a particular emphasis on the critical role of optimizers. Although Adam [14] and AdamW [26] are still the dominant optimizers, numerous efficient optimizers have been proposed to reduce the computing or memory cost of large-scale pre-training [14, 26, 23, 11, 36, 34, 18, 19, 30, 17, 20, 29].

Recently, the Muon optimizer [11] has shown promising performance in pre-training. The key idea of Muon is to orthogonalize the momentum matrix via Newton–Schulz iterations, a scheme designed to effectively counteract gradient rank collapse. Recent research [24] has also validated the scalability of Muon for massive foundation models. This scalability has led to its widespread adoption; Muon is now integral to the pre-training of leading models like Kimi and GLM [32, 5, 37, 33], delivering tangible performance gains. Furthermore, a growing body of literature continues to investigate Muon across various dimensions, including its efficiency, scalability, effectiveness, and theoretical interpretability [39, 3, 13, 2, 21, 15].

In this work, we take one further step toward improving Muon for large-scale pre-training by proposing MUON+, which augments Muon with a simple normalization step applied after the orthogonalization. We conduct extensive pre-training experiments across a range of model scales and large token-to-parameter (T2P) ratios. Despite its simplicity, this modification leads to consistent and substantial performance gains, improving optimization stability and final model quality across all evaluated settings (see Figure 1).

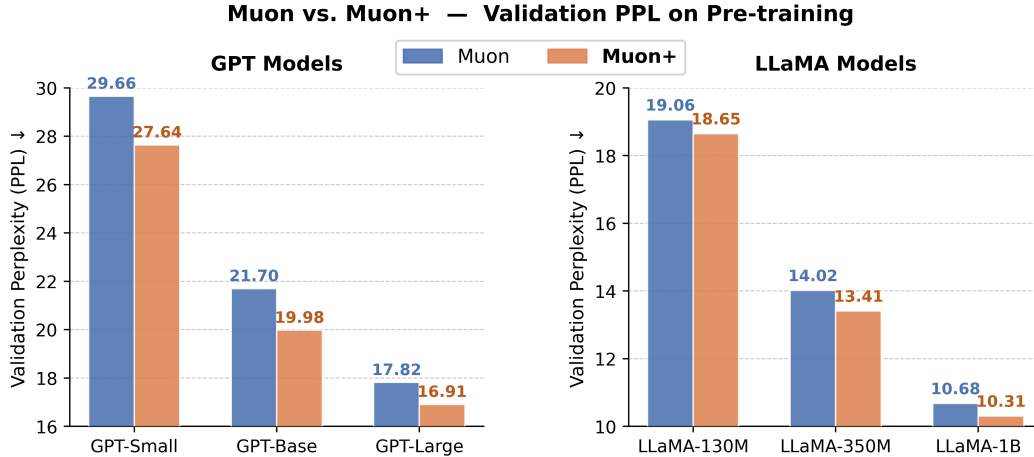


Figure 1: Pre-training GPT and LLaMA models at scales ranging from 130M to 1B parameters under compute-optimal settings. Quantitative results are provided in Section 4. **MUON+** consistently outperforms **MUON** across all runs. We also conduct overtraining experiments for both GPT and LLaMA; the results are presented in Section 4.3.

2 Background

Muon Optimizer Unlike Adam/SGD-based optimizers, Muon [11] operates on a matrix rather than a vector. By enforcing orthogonalization on the layer-wise gradient, Muon prevents the rank collapse of the gradient by replacing the singular value matrix with an identity matrix. Let η and μ denote the learning rate and the momentum coefficient, respectively. Assume that $\mathbf{W}_t \in \mathbb{R}^{m \times n}$ is the layer being adapted at iteration t , $\mathbf{G}_t \in \mathbb{R}^{m \times n}$ is its stochastic gradient, and \mathbf{M}_t is the gradient momentum at iteration t . The Muon update is given by

$$\begin{aligned}
 \mathbf{M}_t &= \mu \mathbf{M}_{t-1} + (1 - \mu) \mathbf{G}_t \\
 \mathbf{O}_t &= \text{Ortho}(\mathbf{M}_t) \\
 \mathbf{W}_t &= \mathbf{W}_{t-1} - \eta \cdot \sqrt{m/n} \cdot \mathbf{O}_t
 \end{aligned} \tag{1}$$

where $\text{Ortho}(\cdot)$ denotes the semi-orthogonal matrix function closest to the input matrix [9]. Specifically, if the SVD of the input matrix \mathbf{M} is $\mathbf{M} = \mathbf{U}\mathbf{\Sigma}\mathbf{V}^T$, then $\text{Ortho}(\mathbf{M}) := \mathbf{U}\mathbf{V}^T$. In practice, the Newton-Schulz iteration process [9] is commonly used to approximate the SVD. The dimensional pre-factor $\sqrt{m/n}$ was suggested by [3] for better scalability. In addition, some variants have been explored to improve the accuracy and speed of this approximation [2, 4].

Remark on the role of normalization. Several recent works introduce additional modifications on top of Muon, such as neuron-wise adaptive scaling (NorMuon[21]) or manifold-inspired updates (Maon[7]), which also involve a normalization step after orthogonalization. Through controlled ablations (See Appendix C), we find that a substantial portion of the observed performance gain can already be attributed to this normalization itself, while the additional components (e.g., second-moment adaptation or manifold formulations) provide comparatively smaller improvements in our pre-training settings.

This observation suggests an alternative interpretation: the key driver of performance improvement may lie in the structural normalization of the orthogonal updates. Motivated by this, we focus on studying normalization and its role in optimization stability during large-scale pre-training, with the goal of identifying normalization strategies that are most suitable for pre-training regimes.

3 The MUON+ Method

MUON+ follows the Muon update rule in Eq. (1) with an additional normalization applied to the orthogonalized update. The update is defined as

$$\begin{aligned}\mathbf{M}_t &= \mu\mathbf{M}_{t-1} + (1 - \mu)\mathbf{G}_t, \\ \mathbf{O}_t &= \text{Norm}_{(d)}(\text{Ortho}(\mathbf{M}_t)), \\ \mathbf{W}_t &= \mathbf{W}_{t-1} - \eta \cdot \sqrt{m/n} \cdot \mathbf{O}_t,\end{aligned}\tag{2}$$

where $\text{Norm}_{(d)}(\cdot)$ denotes a normalization operator applied along direction d . We provide the pseudocode as in Algorithm. 1.

Algorithm 1 Python code for the MUON+ update.

```

1 def muon_plus_step(W, M_prev, G, mu, lr, d="col", eps=1e-8):
2     # momentum
3     M = mu * M_prev + (1.0 - mu) * G
4     # orthogonalize
5     U = Ortho(M) # newton-schulz
6     # normalize
7     O = norm_dir(U, d=d, eps=eps)
8     # update
9     m, n = W.shape[-2], W.shape[-1]
10    W = W - lr * (m / n) ** 0.5 * O
11    return W, M
12
13 def norm_dir(X, d="col", eps=1e-8):
14     if d == "col":
15         denom = (X.square().sum(dim=-2, keepdim=True) + eps).sqrt()
16         return X / denom
17     if d == "row":
18         denom = (X.square().sum(dim=-1, keepdim=True) + eps).sqrt()
19         return X / denom
20     if d == "col_row":
21         return norm_dir(norm_dir(X, "col", eps), "row", eps)
22     if d == "row_col":
23         return norm_dir(norm_dir(X, "row", eps), "col", eps)

```

Specifically, we consider the following normalization directions:

- Column-wise normalization: $\text{Norm}_{(\text{col})}(\cdot)$
- Row-wise normalization: $\text{Norm}_{(\text{row})}(\cdot)$

Let $\mathbf{X} = [x_{ij}] \in \mathbb{R}^{m \times n}$ and $\varepsilon > 0$. The column-wise and row-wise ℓ_2 normalizations are defined as

$$\text{Norm}_{(\text{col})}(\mathbf{X}) := \mathbf{X} \mathbf{D}_{\text{col}}^{-1},\tag{3}$$

$$\mathbf{D}_{\text{col}} := \text{diag} \left(\sqrt{\sum_{i=1}^m x_{i1}^2}, \dots, \sqrt{\sum_{i=1}^m x_{in}^2} \right),\tag{4}$$

and

$$\text{Norm}_{(\text{row})}(\mathbf{X}) := \mathbf{D}_{\text{row}}^{-1} \mathbf{X},\tag{5}$$

$$\mathbf{D}_{\text{row}} := \text{diag} \left(\sqrt{\sum_{j=1}^n x_{1j}^2}, \dots, \sqrt{\sum_{j=1}^n x_{mj}^2} \right).\tag{6}$$

For composed normalization directions, we define

$$\text{Norm}_{(\text{col_row})}(\mathbf{X}) := \text{Norm}_{(\text{row})}(\text{Norm}_{(\text{col})}(\mathbf{X})),\tag{7}$$

$$\text{Norm}_{(\text{row_col})}(\mathbf{X}) := \text{Norm}_{(\text{col})}(\text{Norm}_{(\text{row})}(\mathbf{X})).\tag{8}$$

4 Experiments

We evaluate MUON+ on two widely adopted architectures: GPT and LLaMA. Our evaluation covers both compute-optimal pre-training and long-horizon overtraining regimes, followed by systematic ablation studies on normalization directions, learning rates, and polar approximations in Section 5. Note that, all the experiments in this paper use 5 iterations in Ortho(\cdot) to approximate UV^T .

4.1 Pre-training GPT

Model	Param (M)	Train Tokens (B)	Muon	MUON+
GPT-Small	124	3.0	29.66	27.64 (-2.02)
GPT-Base	362	7.2	21.70	19.98 (-1.72)
GPT-Large	774	15.5	17.82	16.91 (-0.91)

Table 1: Validation PPL of Muon vs. MUON+ on GPT models.

We first evaluate MUON+ on GPT-style models. We pre-train GPT-Small, GPT-Base, and GPT-Large with a token-to-parameter (T2P) ratio of approximately 20. All models are trained on the FineWeb dataset [28], tokenized using the GPT tokenizer, with a vocabulary size of 50,257 and a batch size of 512. Training is conducted on H100/A100 GPUs using mixed precision (bfloat16). Following the setup in [2], we apply MUON+ (or Muon) to all parameters except embeddings, unembeddings, normalization layers, and positional encodings, which are optimized using AdamW. For the polar operator, we adopt the same configuration as in [11]. We sweep normalization directions under learning rates in [0.003, 0.005, 0.01, 0.02, 0.04] for both MUON+ and Muon, and report the best results in Table 1. Detailed hyperparameters and full sweep results are provided in Appendix A and Appendix B.

As shown in Table 1, MUON+ consistently outperforms Muon across all GPT model scales. The improvement is substantial for GPT-Small and GPT-Base, with validation perplexity reductions of 2.02 and 1.72, respectively, and remains significant for GPT-Large with a gain of 0.91.

4.2 Pre-training LLaMA

Model	Param (M)	Train Tokens (B)	AdamW	Muon	MUON+
LLaMA-60M	58	1.1	33.10	25.75	25.25 (-0.50)
LLaMA-130M	134	2.2	23.64	19.06	18.65 (-0.41)
LLaMA-350M	368	6.4	16.18	14.02	13.41 (-0.61)
LLaMA-1B	1339	13.1	14.38	10.68	10.31 (-0.37)

Table 2: Validation PPL of Muon vs. MUON+ on LLaMA models.

To extend our evaluation beyond GPT architectures, we benchmark our proposed approach against AdamW and Muon by pre-training LLaMA-based language models. This validation is also conducted on the FineWeb dataset, spanning model capacities from 60M up to 1B parameters (architectural details are provided in Table 8).

Based on the compute-optimal scaling guidelines established by [10], we strictly pair model sizes with training token budgets: the 60M, 130M, 350M, and 1B parameter models are trained on 1.1B, 2.2B, 6.4B, and 13.1B tokens, respectively. Across all configurations, we maintain a constant batch size of 512 and employ the LLaMA-2 tokenizer with a 32,000-token vocabulary. In line with the setup described in Section 4.1, all experiments are executed using mixed precision on H100 and A100 GPUs.

We sweep normalization directions under learning rates in [0.005, 0.01, 0.02, 0.04, 0.06, 0.08] for all models in this section (see the analysis in Section 5.2). Due to computational constraints, we do not evaluate all normalization directions for the LLaMA-1B model. Instead, we only sweep the *col-row* and *row-col* variants across different learning rates based on the experiment results of smaller models. The best results are reported in Table 2. Additional hyperparameter details are provided in

Appendix A. Overall, as shown in Table 2, MUON+ consistently outperforms the baselines, achieving the best overall performance across all evaluated scales.

4.3 Overtraining GPT and LLaMA

To evaluate the scalability of MUON+ as the number of training tokens increases, we conduct overtraining experiments on GPT-Base and LLaMA-350M. Specifically, both models are trained with a token-to-parameter ratio of approximately 200.

Overtraining GPT We perform an overtraining experiment on GPT-Base to assess the scalability of MUON+ relative to Muon under substantially increased training data. In this setting, GPT-Base is trained with 72 billion tokens from the FineWeb dataset. We use a sequence length of 4096 and a batch size of 512. Detailed hyperparameters are provided in Appendix A.

Model	Param (M)	Train Tokens (B)	Muon	MUON+
GPT-Base	362	72	16.97	15.84 (-1.13)

Table 3: Overtraining GPT-Base. We train GPT-Base with 72 billion FineWeb tokens.

As shown in Table 3, MUON+ consistently outperforms Muon under the overtraining setting. Even when the number of training tokens is substantially increased, MUON+ maintains lower validation perplexity and exhibits more stable optimization behavior. This suggests that the benefit of the additional normalization is not confined to compute-optimal regimes, but persists when models are trained with a substantially large token-to-parameter ratio.

We also provide the training loss curve in Figure 2. The performance gap remains stable throughout training, indicating that MUON+ scales favorably with increased training tokens and does not degrade in later optimization stages. These findings demonstrate the robustness and scalability of MUON+ for long-horizon pre-training.

Overtraining LLaMA Same as GPT-Base, we conduct an 72 billion tokens overtraining experiment on LLaMA-350M.

Model	Param (M)	Train Tokens (B)	Muon	MUON+
LLaMA-350M	368	72	11.48	11.03 (-0.45)

Table 4: Overtraining LLaMA-350M. We train LLaMA-350M with 72 billion FineWeb tokens.

As shown in Table 4, MUON+ again outperforms Muon under the extended training regime. The consistent improvement across these distinct model families suggests that the benefit of the additional normalization is not architecture-specific.

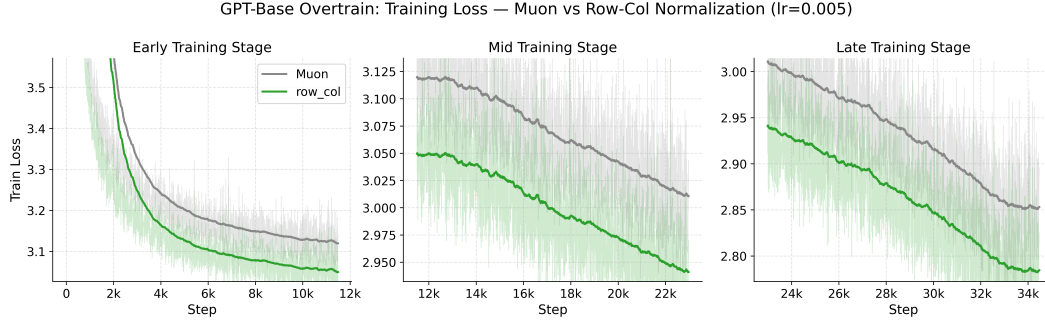
5 Ablation Study

To better understand the source of performance gains, we conduct systematic ablations on the key design choices of MUON+. In particular, we analyze the effects of learning rate, normalization directions, and orthogonalization methods while keeping all other training settings fixed.

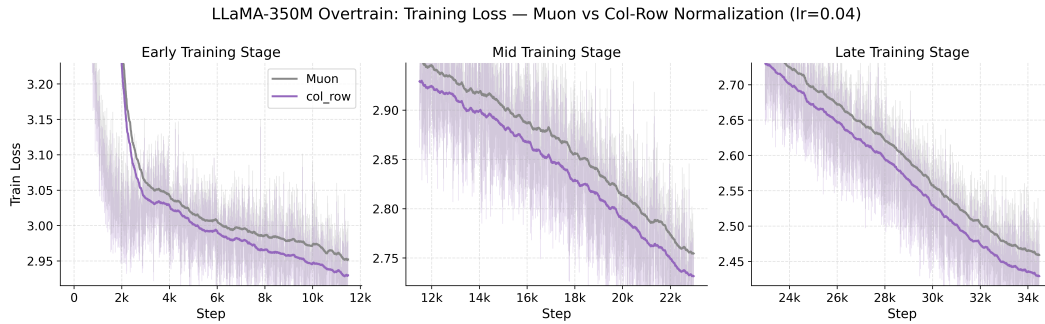
5.1 Performance under Different Learning Rates

To study the sensitivity of MUON+ with respect to the learning rate, we conduct a sweep over a wide range of values and compare it with Muon. We evaluate multiple model scales under identical training configurations, varying only the learning rate. Figure 3 shows the resulting validation perplexity trends, and more detailed sweep results are provided in Appendix B.

Compared with Muon, MUON+ maintains stable performance across a broader range of learning rates for larger models. In particular, when larger models are trained with suboptimal (overly large)

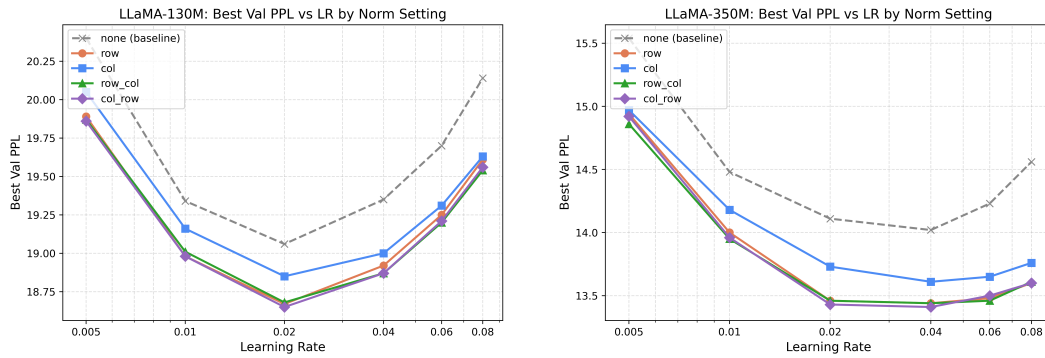


(a) Overtraining GPT-Base



(b) Overtraining LLaMA-350M

Figure 2: Training loss curves under overtraining for GPT-Base and LLaMA-350M.



(a) LLaMA-130M

(b) LLaMA-350M

Figure 3: Validation perplexity sweep for LLaMA models under different settings. Here “none (baseline)” is the standard Muon optimizer; “row”, “col”, “row_col” and “col_row” indicate different normalization directions in MUON+.

learning rates, MUON+ exhibits significantly smaller performance degradation than Muon (Figure 3b). The optimal learning rate for MUON+ is generally comparable to that of Muon, suggesting that the proposed normalization does not require retuning the learning-rate schedule.

Overall, these results indicate that MUON+ not only improves final performance but also reduces sensitivity to learning-rate selection.

Model	None	Col	Row	Col-Row	Row-Col
LLaMA-60M	25.75	25.34	25.29	25.27	25.25
LLaMA-130M	19.34	19.16	18.98	18.65	18.68
LLaMA-350M	14.11	13.73	13.46	13.41	13.44

Table 5: Best validation perplexity under different normalization directions. For each model, we report the best result across learning rates. Lower is better.

5.2 Impact of Different Normalization Directions

We analyze the effect of different normalization directions, including none (Muon Baseline), col, row, col_row, and row_col, across multiple model scales, see Appendix B for more Quantitative results.

Across all evaluated settings, introducing normalization leads to better optimization behavior compared to the baseline Muon without normalization. This improvement maintains as the model scale increases. The two orders (col_row and row_col) behave similarly and yield the best performance. However, there is an asymmetrical behavior between row-wise and column-wise normalization: row consistently achieves better performance than col.

5.3 Ablation for Polar Methods Ortho(\cdot)

To validate the robustness of MUON+ under different polar functions, we adopt 3 different methods (all with 5 iterations) in this section: You [35], Jordan [11], and a more recent method, PolarExpress [2]. Hyperparameters are identical as in Table 11.

Model	Ortho(\cdot)	AdamW	Muon	MUON+
LLaMA-350M	You		14.01	13.38(-0.63)
	Jordan	16.18	14.02	13.41(-0.61)
	PolarExpress		13.90	13.27(-0.63)

Table 6: Validation perplexity comparison among AdamW, Muon, and MUON+ on LLaMA-350M trained for 6.4 billion tokens; all orthogonalization methods use 5 iterations. For MUON+, we use col_row for all runs.

As shown in Table 6, MUON+ consistently outperforms Muon across all evaluated SVD approximation methods. The improvement is observed for both classical approximations such as You and Jordan, as well as the more recent PolarExpress method. Moreover, the relative performance gain remains stable despite differences in approximation accuracy and numerical properties among these methods. These results demonstrate that the effectiveness of MUON+ is largely orthogonalization-agnostic.

6 Conclusion

In this work, we have proposed MUON+ and systematically studied the effect of introducing an additional normalization step after Muon orthogonalization. We have presented comprehensive pre-training results and ablation studies across multiple model architectures, covering token-to-parameter ratios ranging from 20 to 200. Empirical results have shown that MUON+ consistently improves optimization performance and remains effective for long-horizon pre-training across architectures and training regimes.

References

- [1] J. Achiam, S. Adler, S. Agarwal, L. Ahmad, I. Akkaya, F. L. Aleman, D. Almeida, J. Altenschmidt, S. Altman, S. Anadkat, et al. Gpt-4 technical report. *arXiv preprint arXiv:2303.08774*, 2023.
- [2] N. Amsel, D. Persson, C. Musco, and R. M. Gower. The polar express: Optimal matrix sign methods and their application to the muon algorithm. *arXiv preprint arXiv:2505.16932*, 2025.
- [3] J. Bernstein. Deriving muon, 2025.
- [4] F. L. Cesista, Y. Jiacheng, and K. Jordan. Squeezing 1-2
- [5] D. Ding, Z. Ju, Y. Leng, S. Liu, T. Liu, Z. Shang, K. Shen, W. Song, X. Tan, H. Tang, et al. Kimi-audio technical report. *arXiv preprint arXiv:2504.18425*, 2025.
- [6] A. Grattafiori, A. Dubey, A. Jauhri, A. Pandey, A. Kadian, A. Al-Dahle, A. Letman, A. Mathur, A. Schelten, A. Vaughan, et al. The llama 3 herd of models. *arXiv preprint arXiv:2407.21783*, 2024.
- [7] Y. Gu and Z. Xie. Mano: Restriking manifold optimization for llm training. *arXiv preprint arXiv:2601.23000*, 2026.
- [8] A. Han, J. Li, W. Huang, M. Hong, A. Takeda, P. K. Jawanpuria, and B. Mishra. Sltrain: a sparse plus low rank approach for parameter and memory efficient pretraining. *Advances in Neural Information Processing Systems*, 37:118267–118295, 2024.
- [9] N. J. Higham. *Functions of matrices: theory and computation*. SIAM, 2008.
- [10] J. Hoffmann, S. Borgeaud, A. Mensch, E. Buchatskaya, T. Cai, E. Rutherford, D. de Las Casas, L. A. Hendricks, J. Welbl, A. Clark, et al. Training compute-optimal large language models. In *Proceedings of the 36th International Conference on Neural Information Processing Systems*, pages 30016–30030, 2022.
- [11] K. Jordan, Y. Jin, V. Boza, J. You, F. Cesista, L. Newhouse, and J. Bernstein. Muon: An optimizer for hidden layers in neural networks, 2024.
- [12] J. Kaplan, S. McCandlish, T. Henighan, T. B. Brown, B. Chess, R. Child, S. Gray, A. Radford, J. Wu, and D. Amodei. Scaling laws for neural language models. *arXiv preprint arXiv:2001.08361*, 2020.
- [13] A. Khaled, K. Ozkara, T. Yu, M. Hong, and Y. Park. Muonbp: Faster muon via block-periodic orthogonalization. *arXiv preprint arXiv:2510.16981*, 2025.
- [14] D. P. Kingma. Adam: A method for stochastic optimization. *arXiv preprint arXiv:1412.6980*, 2014.
- [15] D. Kovalev. Understanding gradient orthogonalization for deep learning via non-euclidean trust-region optimization. *arXiv preprint arXiv:2503.12645*, 2025.
- [16] T. Kumar, Z. Ankner, B. F. Spector, B. Bordelon, N. Muennighoff, M. Paul, C. Pehlevan, C. Re, and A. Raghunathan. Scaling laws for precision. In *The Thirteenth International Conference on Learning Representations*, 2025.
- [17] X. Li. Black box lie group preconditioners for sgd, 2022.
- [18] X.-L. Li. Preconditioned stochastic gradient descent. *IEEE Transactions on Neural Networks and Learning Systems*, 29(5):1454–1466, May 2018.
- [19] X.-L. Li. Preconditioner on matrix lie group for sgd, 2018.
- [20] X.-L. Li. Stochastic hessian fittings with lie groups, 2024.
- [21] Z. Li, L. Liu, C. Liang, W. Chen, and T. Zhao. Normuon: Making muon more efficient and scalable. *arXiv preprint arXiv:2510.05491*, 2025.

- [22] A. Liu, B. Feng, B. Xue, B. Wang, B. Wu, C. Lu, C. Zhao, C. Deng, C. Zhang, C. Ruan, et al. Deepseek-v3 technical report. *arXiv preprint arXiv:2412.19437*, 2024.
- [23] H. Liu, Z. Li, D. L. W. Hall, P. Liang, and T. Ma. Sophia: A scalable stochastic second-order optimizer for language model pre-training. In *The Twelfth International Conference on Learning Representations*, 2024.
- [24] J. Liu, J. Su, X. Yao, Z. Jiang, G. Lai, Y. Du, Y. Qin, W. Xu, E. Lu, J. Yan, et al. Muon is scalable for llm training. *arXiv preprint arXiv:2502.16982*, 2025.
- [25] Z. Liu, R. Zhang, Z. Wang, M. Yan, Z. Yang, P. D. Hovland, B. Nicolae, F. Cappello, S. Tang, and Z. Zhang. Cola: Compute-efficient pre-training of llms via low-rank activation. In *Proceedings of the 2025 Conference on Empirical Methods in Natural Language Processing*, pages 4627–4645, 2025.
- [26] I. Loshchilov and F. Hutter. Decoupled weight decay regularization. *arXiv preprint arXiv:1711.05101*, 2017.
- [27] F. Mehmood, S. Ahmad, and T. K. Whangbo. An efficient optimization technique for training deep neural networks. *Mathematics*, 11(6):1360, 2023.
- [28] G. Penedo, H. Kydlíček, A. Lozhkov, M. Mitchell, C. A. Raffel, L. Von Werra, T. Wolf, et al. The fineweb datasets: Decanting the web for the finest text data at scale. *Advances in Neural Information Processing Systems*, 37:30811–30849, 2024.
- [29] T. Pethick, W. Xie, K. Antonakopoulos, Z. Zhu, A. Silveti-Falls, and V. Cevher. Training deep learning models with norm-constrained lmos, 2025.
- [30] O. Pooladzandi and X.-L. Li. Curvature-informed sgd via general purpose lie-group preconditioners, 2024.
- [31] G. Team, R. Anil, S. Borgeaud, J.-B. Alayrac, J. Yu, R. Soricut, J. Schalkwyk, A. M. Dai, A. Hauth, K. Millican, et al. Gemini: a family of highly capable multimodal models. *arXiv preprint arXiv:2312.11805*, 2023.
- [32] K. Team, Y. Bai, Y. Bao, G. Chen, J. Chen, N. Chen, R. Chen, Y. Chen, Y. Chen, Y. Chen, et al. Kimi k2: Open agentic intelligence. *arXiv preprint arXiv:2507.20534*, 2025.
- [33] K. Team, A. Du, B. Yin, B. Xing, B. Qu, B. Wang, C. Chen, C. Zhang, C. Du, C. Wei, et al. Kimi-vl technical report. *arXiv preprint arXiv:2504.07491*, 2025.
- [34] N. Vyas, D. Morwani, R. Zhao, I. Shapira, D. Brandfonbrener, L. Janson, and S. M. Kakade. SOAP: Improving and stabilizing shampoo using adam. In *The Thirteenth International Conference on Learning Representations*, 2025.
- [35] Y. You, J. Li, S. Reddi, J. Hseu, S. Kumar, S. Bhojanapalli, X. Song, J. Demmel, K. Keutzer, and C.-J. Hsieh. Large batch optimization for deep learning: Training bert in 76 minutes. *arXiv preprint arXiv:1904.00962*, 2019.
- [36] H. Yuan, Y. Liu, S. Wu, X. Zhou, and Q. Gu. Mars: Unleashing the power of variance reduction for training large models, 2024.
- [37] A. Zeng, X. Lv, Q. Zheng, Z. Hou, B. Chen, C. Xie, C. Wang, D. Yin, H. Zeng, J. Zhang, et al. Glm-4.5: Agentic, reasoning, and coding (arc) foundation models. *arXiv preprint arXiv:2508.06471*, 2025.
- [38] R. Zhang, Z. Liu, Z. Wang, and Z. Zhang. Lax: Boosting low-rank training of foundation models via latent crossing. *arXiv preprint arXiv:2505.21732*, 2025.
- [39] R. Zhang, Y. Zhao, Z. Liu, Z. Wang, D. Li, Y. Su, S. Liu, and Z. Zhang. Teon: Tensorized orthonormalization beyond layer-wise muon for large language model pre-training. *arXiv preprint arXiv:2601.23261*, 2026.
- [40] J. Zhao, Z. Zhang, B. Chen, Z. Wang, A. Anandkumar, and Y. Tian. Galore: Memory-efficient llm training by gradient low-rank projection. *arXiv preprint arXiv:2403.03507*, 2024.

A Hyperparameter

A.1 Model Configurations

Model	n_{embd}	n_{layer}	n_{head}	Param(M)
GPT-Small	768	12	12	124
GPT-Base	1024	24	16	362
GPT-Large	1280	36	20	774

Table 7: Architecture configurations of GPT models.

Model	n_{embd}	n_{layer}	n_{head}	FFN dim	Param(M)
60M	512	8	8	1376	58
130M	768	12	12	2048	134
350M	1024	24	16	2736	368
1B	2048	24	32	5461	1339

Table 8: Architecture configurations of LLaMA-style models.

A.2 Training Configurations

A.2.1 GPT Models

Model	Hyperparameter	Muon	MUON+
GPT-Small	Sequence length	2048	2048
	Learning rate	0.005	0.01
	Weight decay	0.1	0.1
	Norm _d	–	Col-Row
GPT-Base	Sequence length	4096	4096
	Learning rate	0.005	0.005
	Weight decay	0.1	0.1
	Norm _d	–	Row
GPT-Large	Sequence length	8192	8192
	Learning rate	–	–
	Weight decay	0.1	0.1
	Norm _d	–	–

Table 9: Best training hyperparameters for GPT-Small/Base/Large on FineWeb. Sequence lengths are set to 2048/4096/8192 for Small/Base/Large, respectively. We use Jordan orthogonalization for all runs. We keep the same learning rate scheduler as in NanoGPT: a constant learning rate for the first 40% of training steps followed by a linear decay to zero. Sweeping results are provided in Appendix B.

Model	Hyperparameter	Muon	MUON+
GPT-Base	Learning rate	0.005	0.005
	Weight decay	0.1	0.1
	Norm _d	–	Row-Col

Table 10: Training hyperparameters for overtraining GPT-Base. We train 72 billion FineWeb tokens for each setting. Sequence length is 4096 for both runs.

A.2.2 LLaMA Models

Model	Hyperparameter	Muon	MUON+
LLaMA-60M	Sequence length	1024	1024
	Learning rate	0.06	0.06
	LR scheduler	Cosine	Cosine
	Weight decay	0.1	0.1
	Warmup ratio	0.1	0.1
	Norm _d	–	Row-Col
LLaMA-130M	Sequence length	1024	1024
	Learning rate	0.02	0.02
	LR scheduler	Cosine	Cosine
	Weight decay	0.1	0.1
	Warmup ratio	0.1	0.1
	Norm _d	–	Col-Row
LLaMA-350M	Sequence length	4096	4096
	Learning rate	0.04	0.04
	LR scheduler	Cosine	Cosine
	Weight decay	0.1	0.1
	Warmup ratio	0.1	0.1
	Norm _d	–	Col-Row
LLaMA-1B	Sequence length	4096	4096
	Learning rate	–	–
	LR scheduler	Cosine	Cosine
	Weight decay	0.1	0.1
	Warmup ratio	0.1	0.1
	Norm _d	–	Row-Col

Table 11: Best training hyperparameters for LLaMA on FineWeb. Sequence lengths are set to 1024 for 60M/130M and 4096 for 350M/1B. All runs use Jordan orthogonalization. Norm_(col_row) and Norm_(row_col) yield nearly identical performance. Additional sweeping results are provided in Appendix B.

Model	Hyperparameter	Muon	MUON+
LLaMA-350M	Learning rate	0.04	0.04
	Weight decay	0.1	0.1
	Norm _d	–	Col-Row

Table 12: Training hyperparameters for overtraining LLaMA-350M. We train 72 billion FineWeb tokens for each setting. Sequence length is 4096 for both runs.

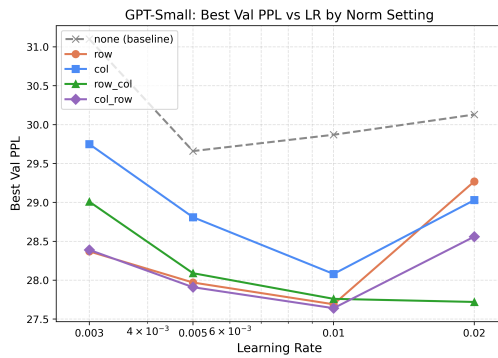
B Detailed Sweep Experiments

LR	None	Col	Row	Col-Row	Row-Col
<i>LLaMA-60M</i>					
0.005	28.98	28.17	28.14	28.10	28.03
0.01	27.03	26.59	26.42	26.46	26.41
0.02	26.22	25.83	25.69	25.65	25.68
0.04	25.90	25.49	25.30	25.28	25.28
0.06	25.75	25.34	25.29	25.25	25.25
0.08	25.97	25.39	25.41	25.29	25.28
<i>LLaMA-130M</i>					
0.005	20.40	20.05	19.89	19.86	19.87
0.01	19.34	19.16	18.98	18.98	19.01
0.02	19.06	18.85	18.67	18.65	18.68
0.04	19.35	19.00	18.92	18.87	18.87
0.06	19.70	19.31	19.25	19.21	19.20
0.08	20.14	19.63	19.61	19.56	19.54
<i>LLaMA-350M</i>					
0.005	15.54	14.97	14.94	14.92	14.86
0.01	14.48	14.18	14.00	13.96	13.95
0.02	14.11	13.73	13.46	13.43	13.46
0.04	14.02	13.61	13.44	13.41	13.44
0.06	14.23	13.65	13.48	13.50	13.46
0.08	14.56	13.76	13.60	13.60	13.61

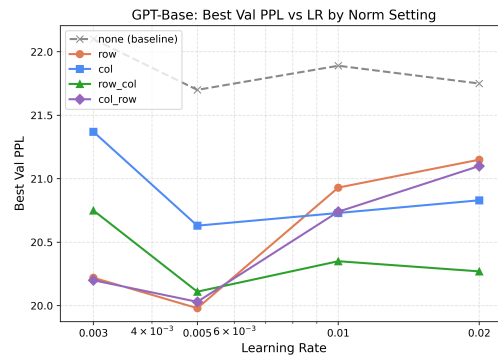
Table 13: Best validation perplexity per norm setting and learning rate for all LLaMA models. Bold marks the best entry in each row. **None** denotes the Muon baseline.

LR	None	Col	Row	Col-Row	Row-Col
<i>GPT-Small</i>					
0.003	31.10	29.75	28.37	28.39	29.01
0.005	29.66	28.81	27.97	27.91	28.09
0.01	29.87	28.08	27.69	27.64	27.76
0.02	30.13	29.03	29.27	28.56	27.72
0.04	30.14	29.71	30.25	30.58	29.37
<i>GPT-Base</i>					
0.003	22.10	21.37	20.22	20.20	20.75
0.005	21.70	20.63	19.98	20.03	20.11
0.01	21.89	20.73	20.93	20.74	20.35
0.02	21.75	20.83	21.15	21.10	20.27
0.04	22.14	23.27	23.16	23.41	22.12

Table 14: Best validation perplexity per norm setting and learning rate for GPT Models. Bold marks the best entry in each row. **None** is the Muon baseline.



(a) GPT-Small



(b) GPT-Base

Figure 4: Validation perplexity sweep for GPT models under different settings.

C Discussion about Other Methods

C.1 Ablation for NorMuon

Model	Muon	MUON+	NorMuon ($\beta_1=0.95, \beta_2=0$)	NorMuon ($\beta_1=0.95, \beta_2=0.95$)
GPT-Small	29.66	27.91	28.29	28.42
GPT-Base	21.70	19.98	20.67	20.72

Table 15: Ablation study isolating the effects of normalization and second-moment scaling. NorMuon with $\beta_2=0$ removes the second-moment term while retaining orthogonalization and normalization, allowing us to disentangle the contribution of normalization from adaptive variance scaling. All variants are trained under the same configuration (learning rate = 0.005). For GPT-Small and GPT-Base, we train on 3B and 7.2B FineWeb tokens, respectively.

NorMuon and the role of second-moment scaling. NorMuon[21] extends Muon by introducing neuron-wise adaptive scaling on top of the orthogonalized updates, aiming to balance update magnitudes across neurons and improve training stability. Specifically, NorMuon maintains a first-order momentum controlled by β_1 and a second-moment estimate controlled by β_2 , where β_1 governs the temporal smoothing of gradients and β_2 controls the adaptive variance-based scaling of update magnitudes.

To understand the contribution of the second-moment term, we conduct a controlled ablation by comparing four settings: Muon, MUON+, NorMuon with $\beta_2 = 0$ (removing second-moment scaling while retaining β_1 and normalization), and NorMuon with $\beta_2 = 0.95$. All methods are evaluated under the same training configuration and learning-rate setting for fair comparison.

As shown in Table 15, removing the second-moment term does not degrade performance and in some cases yields comparable or improved results, while the normalization step consistently provides noticeable gains over the Muon baseline. These results may indicate that the improvement is largely attributable to the normalization step following orthogonalization. The additional second-moment mechanism controlled by β_2 does not yield further benefits.

C.2 Discussion about Mano

The Mano optimizer [7] introduces a reformed manifold optimization tailored for large-scale LLM training. Unlike traditional methods that restrict model parameters to remain on a specific manifold surface, Mano treats the manifold as a soft constraint. Specifically, while the model weights remain in Euclidean space, each update step is projected onto a rotational Oblique manifold (defined by matrices with unit-norm columns or rows). The update involves two primary operations: 1) projecting the momentum onto the tangent space, 2) applying manifold normalization to map that update back to the Oblique surface. Empirically, the authors found that the manifold normalization step is the most critical driver of performance, which essentially is row-wise or column-wise normalization of the update similar to our proposed Muon+. Ablation studies revealed that removing the tangent space projection yielded almost identical results. We argue that the regularization provided by update normalization is the primary factor behind Mano’s superior convergence and stability.